



La Science à l'œuvre pour le
at work for Canada

NRC Publications Archive Archives des publications du CNRC

On the speckle size in optical coherence tomography

Lamouche, Guy; Bisailon, Charles-Étienne; Vergnole, Sébastien;
Monchalain, Jean-Pierre; Gauthier, Bruno

For the publisher's version, please access the DOI link below./ Pour consulter la version de l'éditeur, utilisez le lien DOI ci-dessous.

Publisher's version / Version de l'éditeur:

<http://dx.doi.org/10.1117/12.761862>

Proceedings of SPIE, the International Society for Optical Engineering, 6847, pp. 684724.1-684724.6, 2008

NRC Publications Record / Notice d'Archives des publications de CNRC:

<http://nparc.cisti-icist.nrc-cnrc.gc.ca/npsi/ctrl?action=rtdoc&an=11236141&lang=en>

<http://nparc.cisti-icist.nrc-cnrc.gc.ca/npsi/ctrl?action=rtdoc&an=11236141&lang=fr>

Access and use of this website and the material on it are subject to the Terms and Conditions set forth at

http://nparc.cisti-icist.nrc-cnrc.gc.ca/npsi/jsp/nparc_cp.jsp?lang=en

READ THESE TERMS AND CONDITIONS CAREFULLY BEFORE USING THIS WEBSITE.

L'accès à ce site Web et l'utilisation de son contenu sont assujettis aux conditions présentées dans le site

http://nparc.cisti-icist.nrc-cnrc.gc.ca/npsi/jsp/nparc_cp.jsp?lang=fr

LISEZ CES CONDITIONS ATTENTIVEMENT AVANT D'UTILISER CE SITE WEB.

Contact us / Contactez nous: nparc.cisti@nrc-cnrc.gc.ca.



National Research
Council Canada

Conseil national
de recherches Canada

Canada

On the speckle Size in Optical Coherence Tomography

G. Lamouche, C.-E. Bisailon, S. Vergnole, and J.P. Monchalain

Industrial Materials Institute, National Research Council, Boucherville, Québec, Canada

ABSTRACT

Speckle is always present in Optical Coherence Tomography (OCT) measurements. To a first approximation, the speckle size is determined by the OCT resolution length and the point spread function of the focusing optics in the sample arm. But the speckle size is also affected by the tissue microstructure. We demonstrate this phenomena by performing measurements on optical phantoms with a controlled density of scatterers using time-domain OCT. In the very low density limit, the scatterers are easily identified on the OCT cross-section and, in fact, one can hardly speak of a speckle pattern. The corresponding speckle size is the resolution length axially and the point spread function of the focusing optics transversally. As the number of scatterers increases, a true speckle field appears and the measured speckle size decreases. In the high density limit, the speckle size reaches an asymptotic value that is about 70% of its low-density regime values. In addition to experimental results, theoretical estimates of the limiting speckle size values are presented. Our work contributes to a better understanding of speckle in optical coherence tomography.

Keywords: Optical coherence tomography, speckle, biomedical imaging

1. INTRODUCTION

This paper is about a very simple question: what is the speckle size in images obtained with Optical Coherence Tomography (OCT)? It is common knowledge that the speckle size is influenced by the coherence length of the OCT source and by the optics used for illumination and detection. One can ask if the speckle size is not also related to the sample under study, to its microstructure for example. To investigate if the speckle size is also affected by the microstructure of the sample, we perform experiments on phantoms with different densities of discrete scatterers. We begin in Section 2 by providing boundary values for the speckle size in two limiting regimes: low density of scatterers and high density of scatterers. In Section 3, we provide some details about the experimental work by describing the optical phantoms, the OCT measurements, and the speckle size determination. Speckle size results are then presented in Section 4 for both the axial and transverse directions. In the following, all the speckle size values are Full-Width-at-Half-Maximum (FWHM) values. Additionally, the axial direction corresponds to the depth direction and the transverse direction to the lateral scanning direction.

2. BOUNDARY VALUES FOR THE SPECKLE SIZE

An estimate for the speckle size sometimes found in the literature is provided by the OCT resolution length in the axial direction and the width of the point spread function of the optics in the transverse direction. The latter corresponds to the spot size divided by the squared root of two.¹ These values correspond to the system response for a single scatterer. They are thus valid when there are very few scatterers, i.e., in the low density of scatterer regime. When the number of scatterers increases, summing the coherent contributions of the various scatterers affects the envelope that is obtained in OCT. This problem is very similar to the one considered by Wagner et al.² who evaluated the speckle size in ultrasonic B-scans. For the case where the response of a single scatterer is characterized by a gaussian envelope, the many scatterer regime leads to a speckle size with speckle blobs that are about 30% smaller. Consequently, for the axial speckle size measured in OCT, one should obtain about 70% of the OCT resolution length. This should be valid for all depths. For the transverse speckle size measured in the focal region, one should observe 70% of the width of the point spread function.

The above discussion provides boundary values for the speckle size in two limiting regimes: the low and high density of scatterer regimes. Between these two regimes, the speckle size is expected to evolve monotonically between the boundary values.

Further author information: (Send correspondence to G.L.)
G.L.: E-mail: guy.lamouche@cnrc-nrc.gc.ca, Telephone: 1 450 641 5198

3. EXPERIMENTAL DETAILS

In this section, we provide some experimental details about the optical phantoms, the OCT measurements, and the speckle size determination.

3.1 Optical phantoms

This work asks for optical phantoms with very specific properties. The matrix must be solid and transparent, the scatterers must have known dimensions and shape, and the density of the scatterers must be well controlled. We reviewed existing solutions in the literature and concluded that we needed to develop a new combination of matrix-scatterers to satisfy our needs. We developed phantoms with silica microspheres in a Sylgard 184 silicone matrix. The details of fabrication and resulting characteristics are discussed more at length elsewhere.³ We focus here on the most important property: the controlled density of scatterers. Firstly, Figure 1 shows a phantom along with a Scanning Electron Microscope (SEM) image of its cross-section. The white dots in the SEM image are the microspheres and the dark dots are voids left by microspheres ejected when cutting of the cross-section. From the SEM image, one can appreciate the randomness and homogeneity of the microsphere distribution. Additionally, no aggregates are visible. Secondly, Figure 2 presents the average number of microspheres evaluated over six images taken from a cross-section as a function of the density of scatterers used in the fabrication process. The linearity of the relation between the two variables clearly shows that the phantoms are fabricated with a very well controlled density of scatterers. All the results presented in this paper were obtained with phantoms fabricated with silica microspheres with a diameter of $1.86 \mu\text{m}$.

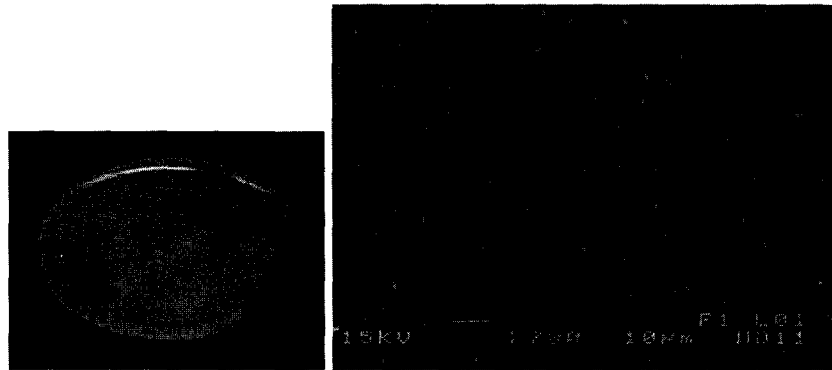


Figure 1. Left image shows a molded phantom used for the experiment. Right image shows a scanning electron microscopy image of the cross-section of a phantom.

3.2 OCT measurements

Measurements are performed with a time-domain OCT (TD-OCT) system that provides an axial resolution of about $14.9 \mu\text{m}$. The focusing optics used in the sample arm provides a spot size of $7.4 \mu\text{m}$, the focal point being located about $300 \mu\text{m}$ below the surface of the optical phantom. The corresponding depth of field is about $90 \mu\text{m}$ in the phantom. Figure 3 shows the measured speckle field for four phantoms with different density of scatterers. The phantoms are identified by an Effective Number of Scatterers (ENS) which is the average number of scatterers contained within the probed volume defined by the coherence length of the source and the spot size. This definition was proposed by Hillman et al.⁴ and our ENS values are evaluated with their peculiar definition of the coherence length. The ENS value will vary with the axial position in the sample since the illuminating spot size varies, so does the probe volume. In Figure 3 and in the following, the phantoms are often identified by a single ENS value that corresponds to the ENS evaluated in the focal region.

For the case with very few scatterers (ENS=0.2) in Figure 3, one can hardly speak of a speckle field since one can clearly identify the individual scatterers. As the density of scatterers increases (larger ENS values), a true speckle field appears with its worm-like structure. From the intensity of the speckle field, one can clearly see in Figure 3 that the focal point lies within the sample. The samples are illuminated from the top in Figure

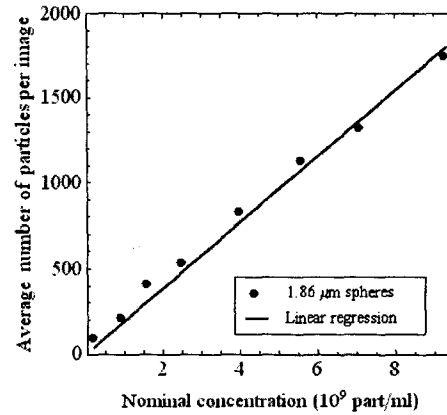


Figure 2. Number of microspheres averaged over six images taken from the cross-section of various phantoms as a function of the density of scatterers used in the fabrication process.

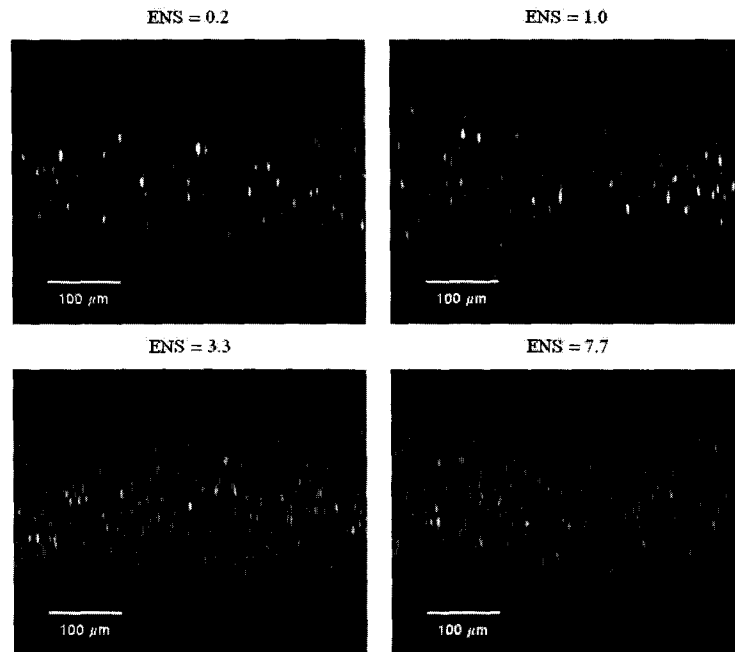


Figure 3. Measured TD-OCT speckle fields for various phantoms identified by their ENS value (see text) evaluated in the focal region.

3. To reduce the effect of the strong reflection at the air-sample interface (not shown in Figure 3), the samples were slightly inclined during the measurement.

3.3 Speckle size determination

For the transverse direction, the speckle size is evaluated from the autocorrelation of a rectangular window. Typical dimensions for the window are $50 \mu\text{m}$ in the axial direction and 1.5 mm in the transverse direction. The autocorrelation function is then fitted with a gaussian function from which the width is extracted and converted to provide a FWHM value for the transverse speckle size. To obtain the variation of the speckle size with depth, the processing is simply repeated by positioning the window at various axial positions.

For the axial speckle size, we proceed in a similar manner, but in the axial direction. The window is much shorter in the axial direction. Thus, instead of using an autocorrelation, we correlate the window over another window that is three times larger and centered on the first one. This process is more robust and provides more reliable values. Again, the correlation result is fitted with a gaussian function from which the width is extracted and converted to a FWHM axial speckle size value. The process is repeated again at various positions in the axial direction to provide a depth variation of the speckle size.

4. SPECKLE SIZE RESULTS

The results of the transverse and axial speckle size measurements are presented and discussed.

4.1 Transverse speckle size

Figure 4 presents the measured transverse speckle size in the focal region for various phantoms. The dotted lines represent the upper and lower boundaries evaluated from the discussion presented in Section 2. The higher boundary that corresponds to the low density regime is the width of the point spread function (FWHM) which gives $4.35 \mu\text{m}$. The lower boundary is about 70% of that value which gives $3 \mu\text{m}$. The experimental results in Figure 4 are pretty well contained within these boundaries. For the cases with very low densities of scatterers, the measured values slightly exceed the upper boundary, but this is attributed to experimental uncertainty. The OCT signal is very weak for these cases and the poor signal-to-noise ratio impacts the quality of the speckle size determination. Figure 4 shows that the speckle size indeed decreases as the density of scatterers increases. In the low density regime (low ENS values), one can hardly speak of a speckle field since the scatterers are well separated. For currently available resolutions in OCT and considering that many structures act as scatterers in biological tissues, most of the biological tissues have higher ENS values than the rightmost part of Figure 4.

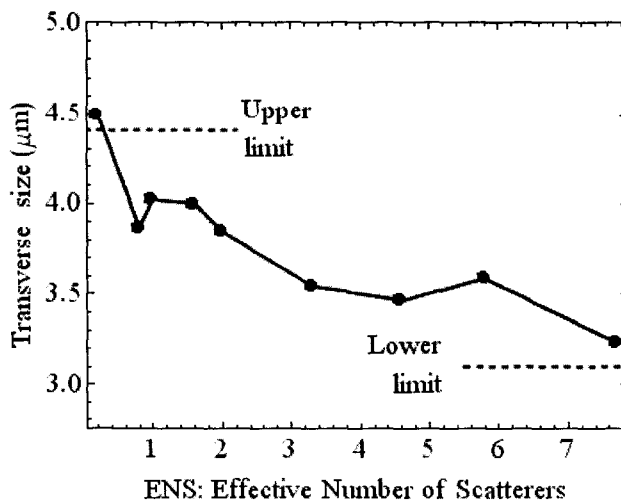


Figure 4. Transverse speckle sizes in the focal region measured for phantoms with different densities of scatterers and identified by their ENS values at the focal point. The dotted lines represent the expected upper and lower boundaries.

Figure 5 presents the evolution of the transverse speckle size away from the focal region. In the low density regime, as we go away from the focal point, the speckle size increases since the illuminating spot size increases. The dotted line illustrates what should be obtained for single scatterers at each depth. The experimental results for the very low ENS values are in good agreement with the expected values. For the large ENS values, there is a lot of scatterers even in the small probed volume near the focal region, providing a smaller speckle size. As we go away from the focal point, the number of scatterers contained in the probed volume further increases but the measured transverse speckle size does not vary much.

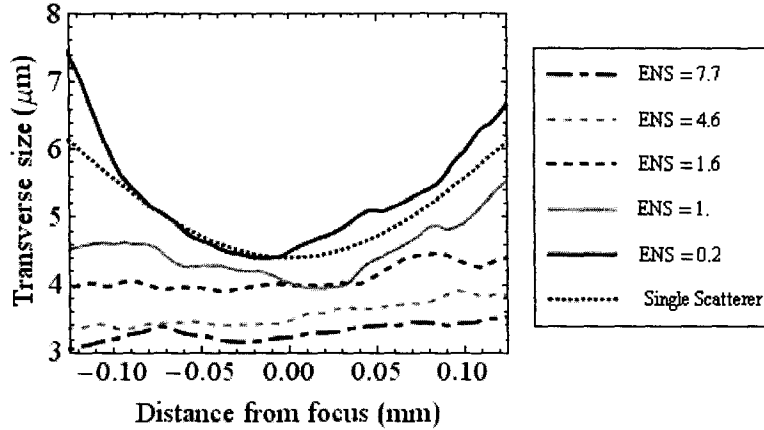


Figure 5. Transverse speckle sizes around the focal point measured for phantoms with different densities of scatterers and identified by their ENS values at the focal point. The dotted line represents the expected variation for a single scatterer.

4.2 Axial speckle size

Figure 6 presents the axial speckle size measured in the focal region for various phantoms. The dotted lines illustrate again the upper and lower expected boundaries. The upper value corresponds to the measured OCT resolution of $14.9 \mu\text{m}$ while the lower value is about 70% of that value at $10.2 \mu\text{m}$. The experimental results in both the low and high density regimes are a little smaller than expected, but the range covered by the values is in quite good agreement with what is predicted. The slight discrepancy is attributed to the larger uncertainty in the axial speckle size since the window used for evaluating the speckle size is rather short. Again, we see that the speckle size decreases as the density of scatterers increases.

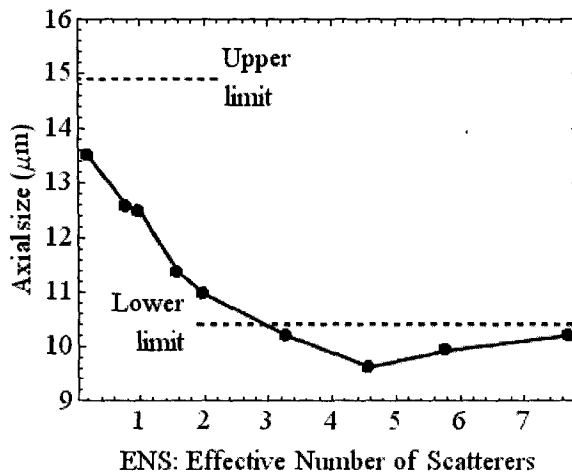


Figure 6. Axial speckle sizes in the focal region measured for phantoms with different densities of scatterers and identified by their ENS values at the focal point. The dotted lines represent the expected upper and lower boundaries.

Figure 7 presents the measured axial speckle size as a function of the position from the focal point. Unlike the transverse case, for low density of scatterers, the speckle size decreases away from the focal point. In that case, the axial envelope function for a single scatterer does not vary with depth and the decrease in speckle size away from the focal point can be solely attributed to the increase of the probed volume, i.e., the increase in the

number of probed scatterers. For the large ENS values, there is essentially no variation in axial speckle size as we go away from the focal point.

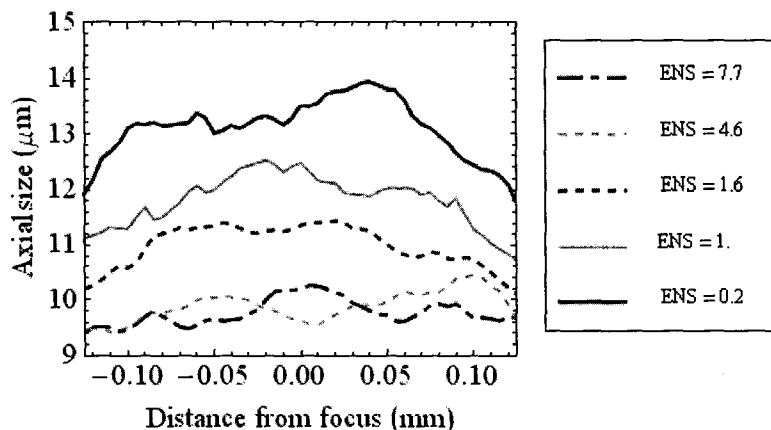


Figure 7. Axial speckle sizes around the focal point measured for phantoms with different densities of scatterers and identified by their ENS values at the focal point.

5. CONCLUSION

We have demonstrated that the speckle size evolves between two limits that are determined by the OCT resolution length and the optics. The speckle size in the focal region in the case of a large number of scatterers is about seventy percent smaller than what can be estimated from the single scatterer response. This is a large variation since in two dimensions the resulting area of a speckle blob is decreased to 50% and in three dimensions its volume is decreased to 35%. This work contributes to a better understanding of speckle and should be of interest to elastography and speckle reduction techniques.

REFERENCES

1. Schmitt, J. M., and Knüttel, A., "Model of optical coherence tomography of heterogeneous tissue," *Journal of the Optical Society of America A* 14(6), 1231-1242 (1997).
2. Wagner, R. F., Smith, S. W., Sandrik, J. M., and Lopez, H., "Statistics of speckle in ultrasound B-scans," *IEEE transactions on sonics and ultrasonics* 30(3), 156-153 (1983).
3. Bisailon, C.E., Lamouche, G., Lanthier, M.M., Lévesque, D., Maciejko, R., and Monchalain, J.P., "Deformable and durable optical phantoms with controlled density of scatterers," to appear in *Photonics West 2008 proceedings, SPIE, San Jose, Paper 6870-10* (2008).
4. Hillman, T. R., Adie, S. G., Seemann, V., Armstrong, J. J., Jacques, S. L., and Sampson, D. D., "Correlation of static speckle with sample properties in optical coherence tomography," *Optics Letters* 31(2), 190-192 (2006).